Experiments on the Performance of a 2-DOF Pantograph Robot Actuated by Shape Memory Alloy Wires

Yee Harn Teh and Roy Featherstone
Department of Information Engineering
Research School of Information Sciences and Engineering
The Australian National University
Canberra ACT 0200
{yee.teh,roy}@rsise.anu.edu.au

Abstract

This paper describes a study of tracking speed and accuracy for a 2-DOF pantograph robotic device actuated by two antagonistic pairs of electrically-heated SMA wires. The objective is to investigate the coupling effect due to the actuation of the two SMA pairs and the dynamics of the pantograph device on the performance of the motion control system. Two different controllers, a two-stage relay controller and a modified proportional controller, have been tested and compared, and experimental results are presented in this paper. The relay controller performs satisfactorily in terms of speed of response, but the large limit cycle phenomenon degrades its accuracy. The modified proportional controller manages to reduce the limit cycle problem and its tracking speed is comparable with the relay controller. Experimental results will also show that the modified proportional controller may not be the best controller for this SMA-actuated pantograph device.

1 Introduction

1.1 Background

Shape memory alloys (SMA) are a group of metallic alloys that have the ability to return to a specific shape or size prior to deformation via a temperature dependent phase change. When these alloys are in the low-temperature phase, the martensite phase, they can be easily deformed. When they are heated through a suitable range of temperatures, the crystal structures transform from martensite to austenite phase and they return to the previous shape. This phase transformation process is known as the shape memory effect and forms the basis of actuation in shape memory alloys.

SMA-based actuators have various uses in robotic research and applications including actuators in active endoscopes [Ikuta *et al.*, 1988], robotic actuators [Mosley and Mavroidis, 2001; Reynaerts and Van Brussel, 1998] and micro-actuators [Troisfontaine *et al.*, 1998; Yao *et al.*, 2004]. They have advantages in terms of mechanical simplicity, high power-to-weight ratio, small size, and silent, spark-free operation. However, they are not free from disadvantages such as inefficiency, limited strain, temperature hysteresis and slow speed. In these applications, the actuators are usually in the form of one or more wires or coils. These SMA actuators are typically coupled with a bias spring or weight to provide actuation opposite to the contraction of the SMA elements, or arranged as antagonistic pairs. They are normally heated by means of joule heating (i.e. passing an electrical current through the element), and cooled by heat transfer to the environment.

1.2 Problem Statement

SMA actuators are generally considered to be slow and inaccurate due to their inherent thermal hysteresis in the phase transformation. Various research and development have been made to improve the performance of SMA elements. In [Elahinia *et al.*, 2004], a single degree-of-freedom (1-DOF) SMA-actuated arm had been used to develop variable structure controllers that are highly accurate in tracking both stationary and variable input signals. Grant [Grant, 1999] proposed the use of specially-constructed SMA coils in antagonistic arrangements using a two-stage relay controller to achieve relatively fast motion control of the actuators. By implementing a rapid heating mechanism in addition to Grant's relay controller, we have managed to further improve the speed of actuation of SMA wire actuators [Featherstone and Teh, 2004; Teh and Featherstone, 2004]. In the second paper, we proposed using a modified proportional controller which successfully reduced the limit cycle which was problematic to a two-stage relay controller design. It should also be noted that these researches had been carried out to investigate the performance of SMA-actuators in 1-DOF robots or mechanisms.

We propose using the controller designs we have imple-

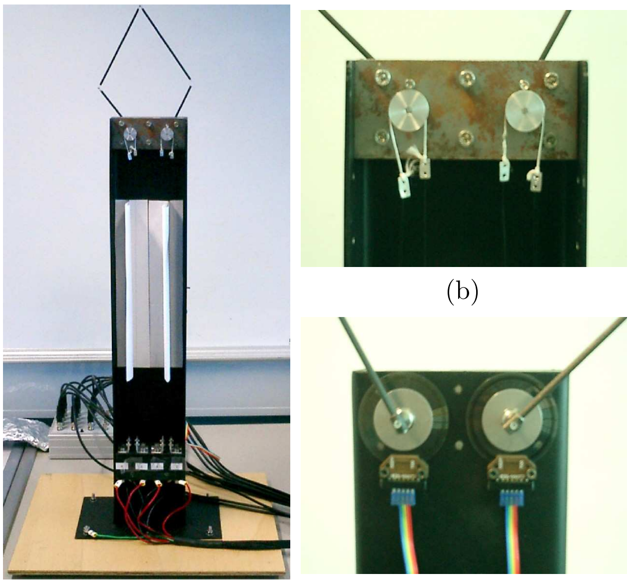

(a) (b) (c)

Figure 1: The experimental rig (a), and detailed views of the pulleys (b) and optical encoders (c).

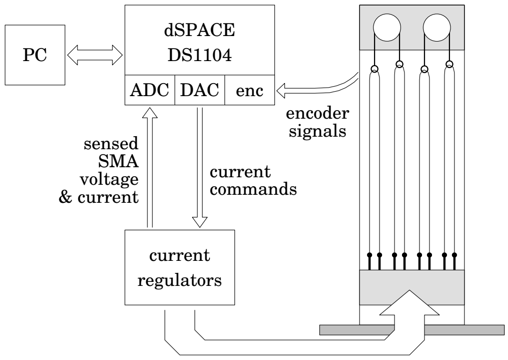

Figure 2: Schematic diagram of experimental hardware.

mented in our previous research to investigate the performance of a 2-DOF pantograph robotic device actuated by two antagonistic pairs of SMA wires. In such a 2-DOF robot, factors such as the coupling effect of the SMA actuators and the external payload due to the weight of the pantograph will affect the speed and accuracy of the motion control system.

1.3 Overview

We have constructed a test rig that houses two antagonistic pairs of SMA wires to actuate a 2-DOF pantograph device. We have extended our motion control system from that described in [Featherstone and Teh, 2004; Teh and Featherstone, 2004] to control both pairs of SMA elements using two different motion controllers. The experimental results are based on a planned trajectory which the tip of the pantograph device attempts to track. This paper describes the experimental hardware, the principle of operation of our motion control system, and the experimental results from the motion controllers comparing the performance between the two controllers.

2 Experimental Setup

2.1 Experimental Hardware

The experimental rig is shown in Figure 1(a) and schematically in Figure 2. It consists of a vertical steel C-beam, about 0.7m high, supporting two horizontal protruding shafts at the top and eight anchor points at the bottom. Each shaft at the top rotates freely on ball bearings and carries a small pulley at the front (Figure 1(b)) and an optical encoder wheel at the rear (Figure 1(c)). The two shafts terminate with small sockets, welded to the rear end of each shaft, which hold the ends of a pantograph linkage made from carbon tubes. This 2-DOF pantograph device serves as the moving robot as well as a mechanical load. In the experiments, the motion control system attempts to move the tip of the pantograph to follow certain trajectories, such as a circle or a square.

Separators made of paper are affixed half way up the column to prevent the SMA elements from making electrical contact with their neighbours if they go slack. A short chord is wrapped around each pulley and is affixed so that it cannot slip relative to the pulley. Each end of the chord terminates with a metal eyelet. Four $100\mu m$-diameter Flexinol wires are strung between the eight anchor points and the eyelets as shown in Figure 2 to form two antagonistic pairs of SMA actuators. These wires are approximately 1 m long and are too thin to be visible in Figure 1(a).

Figure 2 shows a schematic diagram of the complete experimental setup. All real-time computation and data capture functions are performed on a DS1104 board from dSpace, which communicates with a PC in the MATLAB/Simulink environment. Current regulators deliver electrical power to each SMA wire independently, according to signals from the four DAC outputs of the DS1104. Each regulator is capable of supplying more than 0.65A (40W) to its load, which is more than enough to burn out the SMA wires. The actual voltage across each wire and the actual current passing through it can be measured using the current regulator circuits, and these signals are passed back to the ADC inputs on the DS1104.

The optical shaft encoders are also connected to the DS1104 to provide rotation angles of each pulley from an absolute position. Based on this setup, the motion range of the pulley due to the actuation of Flexinol wires is slightly more than 90°.

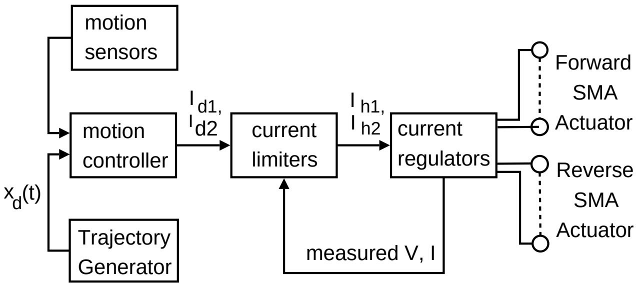

Figure 3: Motion control system for one antagonistic pair of SMA actuator wires.

2.2 The Control System

Figure 3 shows a diagram of the control system for one antagonistic pair of SMA wires incorporating the rapid heating mechanism described in [Featherstone and Teh, 2004; Teh and Featherstone, 2004]. To actuate a 2-DOF robot, the motion control system in Figure 3 is also applied to another antagonistic pair of SMA wires.

The trajectory generator outputs joint space data for the two-dimensional trajectory of the pantograph robot. The speed as well as the shape and size of the trajectory can be specified. The desired joint angle, $x_d(t)$, for each pulley is pre-calculated and forms the input to the motion control system. Using this desired position signal and actual position signals from one of the two encoders, the motion controller determines an output signal for each element, I_{d1} and I_{d2}. These signals can be interpreted as the desired heating currents for the forward and reverse SMA elements. The desired heating currents are passed to a current limiter, which calculates safe heating currents, I_{h1} and I_{h2}, according to the formula:

$$I_{hi} = \min(I_{di}, I_{max}(R_i)), \quad i \in \{1, 2\}, \tag{1}$$

where $I_{max}(R_i)$ is the safe maximum heating current computed according to the rapid heating algorithm described in [Featherstone and Teh, 2004; Teh and Featherstone, 2004], and R_i is the measured electrical resistance of the appropriate SMA wire. In effect, the resistance is being used as an indication of temperature; and the rapid heating algorithm allows a large heating current when the resistance indicates that the wire is not hot, and a smaller, safe heating current otherwise. Without any limit on I_d, there is a risk of overheating the SMA elements. The rapid heating method allows larger heating currents to be applied without risk of overheating.

The current regulators then pass the currents of I_{h1} and I_{h2} through the SMA elements. The actual voltages across the SMA elements and the actual currents through them are measured and sent to the current limiters so that the electrical resistance of both SMA elements can be calculated. However, due to noise in the signals, we found it necessary to pass them through software low-pass filters before we could obtain accurate electrical resistance measurements.

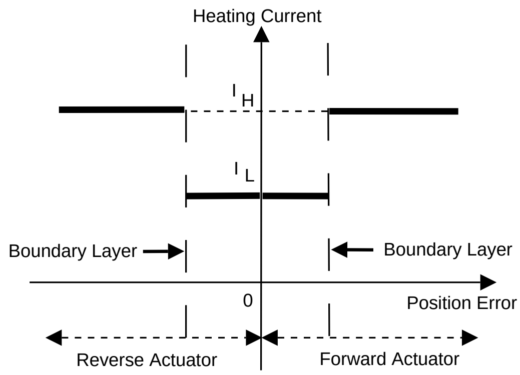

Figure 4: Two-stage relay controller.

We have investigated the behaviour of our rapid heating algorithm with two motion control laws: a two-stage relay controller and a modified proportional controller. Note that the controller designs are described for one antagonistic pair of actuators. In the experiments, they are applied to both antagonistic SMA-pairs to actuate the 2-DOF pantograph robot.

2.3 The Controller Design

Two-Stage Relay Controller

Grant's two-stage relay controller [Grant, 1999] implements the control law scheme as shown in Figure 4. At any instant, only one SMA element of the antagonistic pair is being heated, depending on the sign of the position error. It uses two constant magnitude heating currents to drive the SMA elements. The following control law is implemented:

$$(I_{Fd}, I_{Rd}) = \begin{cases} (0, I_H) & \theta_{err} < -\phi \\ (0, I_L) & -\phi \le \theta_{err} < 0 \\ (I_L, 0) & 0 \le \theta_{err} < \phi \\ (I_H, 0) & \phi \le \theta_{err}, \end{cases} \tag{2}$$

where θ_{err} is the position error, I_{Fd} and I_{Rd} are the desired heating currents for the forward and reverse SMA elements respectively, and I_H, I_L and ϕ are parameters of the controller. When the position error is large, the high current input, I_H, is used to drive the actuator quickly to the desired position. As the position error approaches zero and reaches the boundary layer, ϕ, the relay controller switches to a lower current input, I_L, for smoother and more stable response. The forward and reverse SMA elements pull in the positive and negative directions, as measured by the position sensor. The desired heating currents, I_{Fd} and I_{Rd}, are the inputs to the current limiters which calculate the actual heating currents to be sent to each SMA.

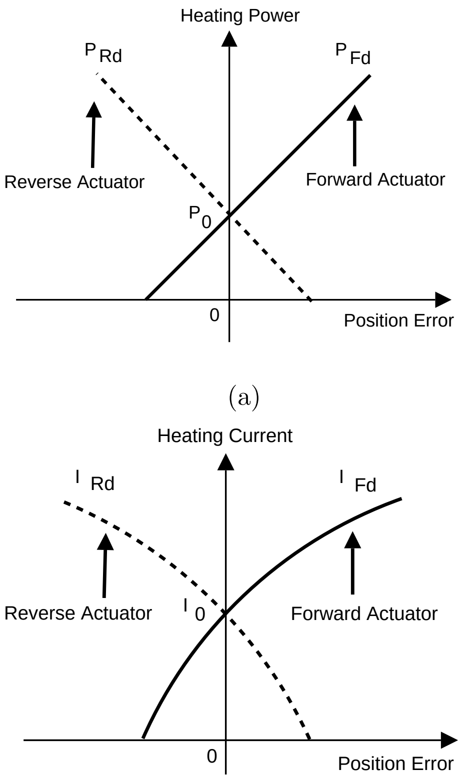

(a)

(b)

Figure 5: Modified proportional controller: heating power vs. position error, θ_{err} (a), and heating current vs. position error, θ_{err} (b).

Note that our two-stage relay controller differs from Grant's on the magnitude of heating currents. Whereas Grant used the safe current level specified in the SMA data sheets as I_H, we set I_H to a value greater than the safe current level, and rely on the current limiter to prevent overheating.

Modified Proportional Controller

The modified proportional controller algorithm is depicted in Figure 5. The controller computes a linear power ramp (Figure 5(a)) and converts the heating power, P, to current, I (Figure 5(b)), based on the following relationship:

$$I = \sqrt{\frac{P}{R_{nom}}}, \tag{3}$$

where R_{nom} is the pre-determined, nominal resistance of the SMA element.

Basically the modified proportional controller implements the following control law:

$$\begin{aligned} P_{Fd} &= \max(0, P_0 + K_p\theta_{err}), \\ P_{Rd} &= \max(0, P_0 - K_p\theta_{err}), \end{aligned} \tag{4}$$

where θ_{err} is the position error, P_{Fd} and P_{Rd} are the desired heating powers for the forward and reverse SMA elements in one antagonistic pair, respectively, K_p is the proportional gain, and P_0 is the applied heating power when θ_{err} is zero. When the error is large, only one wire is heated according to the control law. The other wire in the same antagonistic pair remains cold. As the error decreases, the desired heating power decreases proportionally. At a certain position error, the controller will commence supplying power to the other SMA element so that both actuators are being heated and do not become slack. Depending on the sign of the error, one SMA element is supplied more power than the other, and actuation occurs in the desired direction.

By setting P_0 correctly (by empirical method), both elements will be supplied the same level of heating power, and remain just above the austenite start temperature, when the position error is zero. The rationale is to keep both wires taut when the position error is zero, by keeping both of them warm. This is to eliminate or to further reduce the limit cycle.

3 Experimental Results

The two different controllers have been tested under a variety of conditions. Under the uncoupled condition, one of the pulleys (in our experiments, the left pulley) is completely fixed at one position while the other is free to rotate. In this case, the pantograph only acts as a mechanical load and there is no coupling effect from the fixed linkage. Whereas under the coupled condition, both pulleys are free to rotate and currents are sent to both pairs of SMA wires.

Figures 6, 7 and 8 show, under uncoupled conditions, the tracking responses of the moving pulley actuated by one SMA pair to 0.1 Hz, 0.5 Hz and 1 Hz circular trajectories respectively, where x Hz means that one complete execution of the trajectory takes $1/x$ seconds. The circular trajectory has a 2cm radius. Experiments were carried out using both the two-stage relay controller and the modified proportional controller.

The pantograph linkage constitutes a difficult load to control, as there is no physical damping in the system. The relay controller responses clearly exhibit a serious limit cycle problem caused by the combined behaviour of the control system and the plant. This problem is more prominent at lower frequencies as the controller manages to track the input command and switches between the positive and negative position errors. Figure 9 presents the actual angle errors from the tracking responses in Figure 6, clearly showing the significantly larger limit cycles with the relay controller. Using the modified proportional controller, the large limit cycles have been reduced significantly with careful tuning of

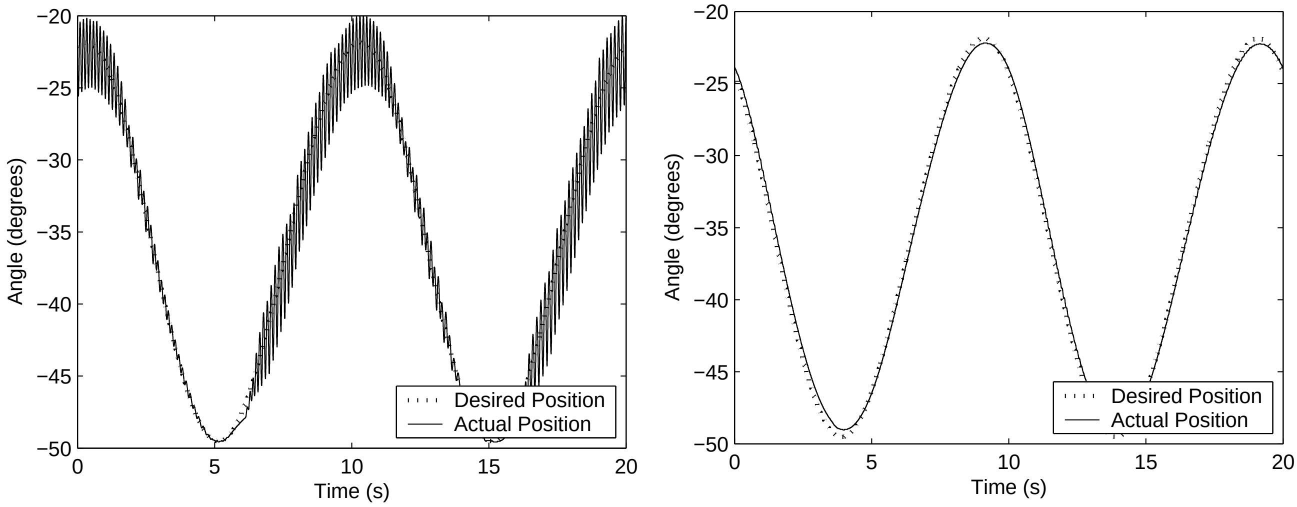

(a) (b)

Figure 6: Tracking response of one antagonistically actuated pulley of the 2-DOF pantograph, with the other pulley locked in a fixed position, to a 0.1 Hz circular motion command, (a) using the relay controller, and (b) the modified proportional controller.

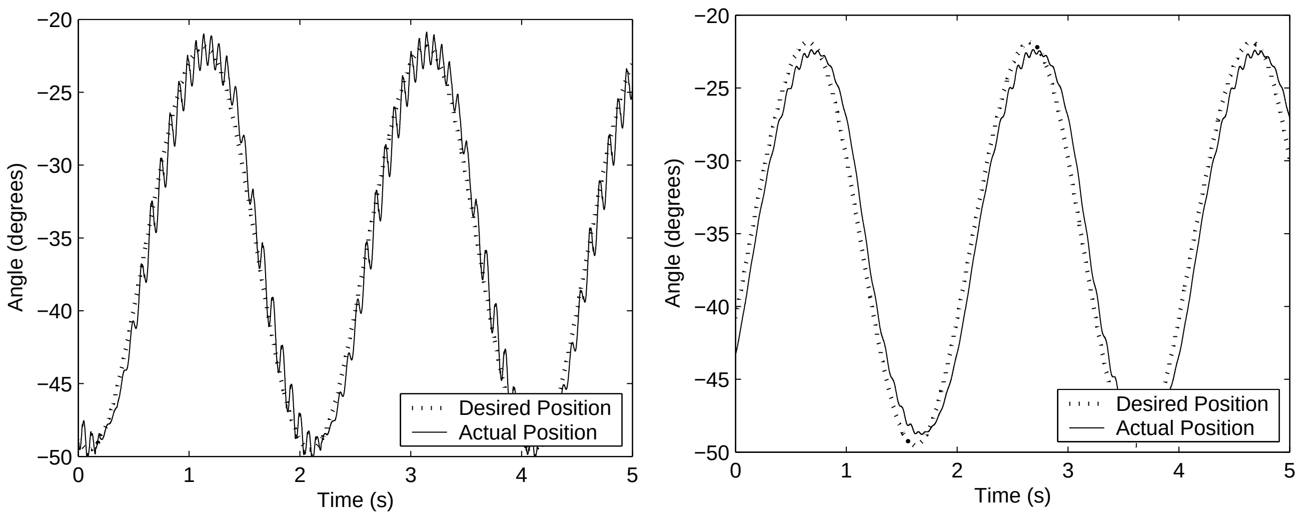

(a) (b)

Figure 7: Tracking response of one antagonistically actuated pulley of the 2-DOF pantograph, with the other pulley locked in a fixed position, to a 0.5 Hz circular motion command, (a) using the relay controller, and (b) the modified proportional controller.

the parameters, K_p and P_0.

Results also show that the modified proportional controller performs similarly or even better than the relay controller in terms of tracking speed at 1 Hz as shown in Figure 8. However, for the modified proportional controller, the maximum currents supplied to the SMA actuators are approximately 10% greater than I_H of the relay controller, therefore resulting in better tracking. Although increasing I_H would allow the relay controller to match the speed of the proportional controller, it would also result in larger limit cycles (from experimental observation).

Figure 10 shows the actual currents delivered to the two SMA wires during the 0.5 Hz tracking response of Figure 7. It is clear, for the two-stage relay controller shown in Figure 10(a), that only one actuator is switched on at any instant depending on the error sign, and there are two distinctive current levels that are delivered to the

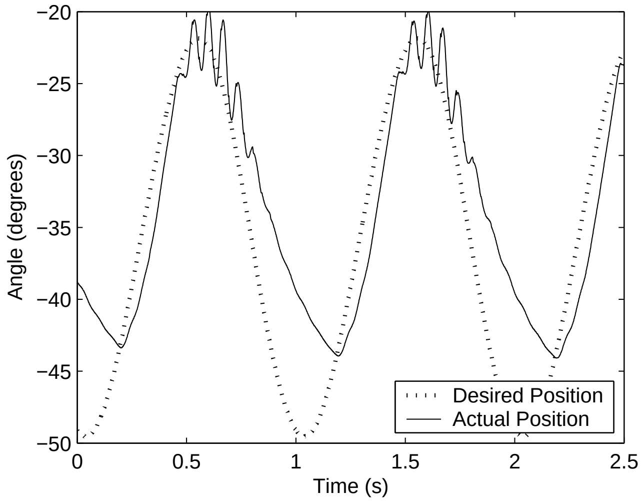

(a)

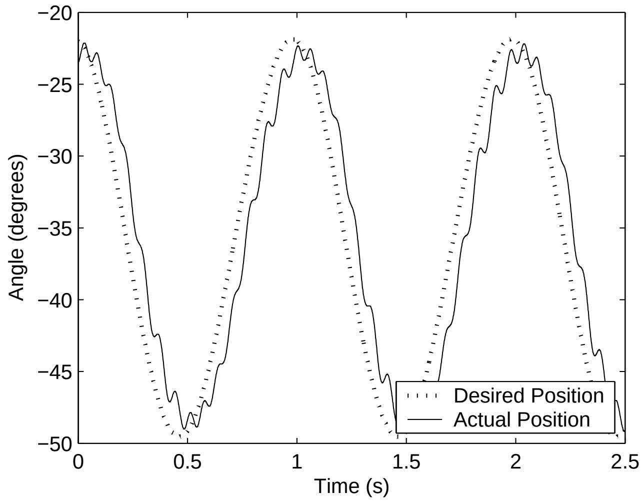

(b)

Figure 8: Tracking response of one antagonistically actuated pulley of the 2-DOF pantograph, with the other pulley locked in a fixed position, to a 1 Hz circular motion command, (a) using the relay controller, and (b) the modified proportional controller.

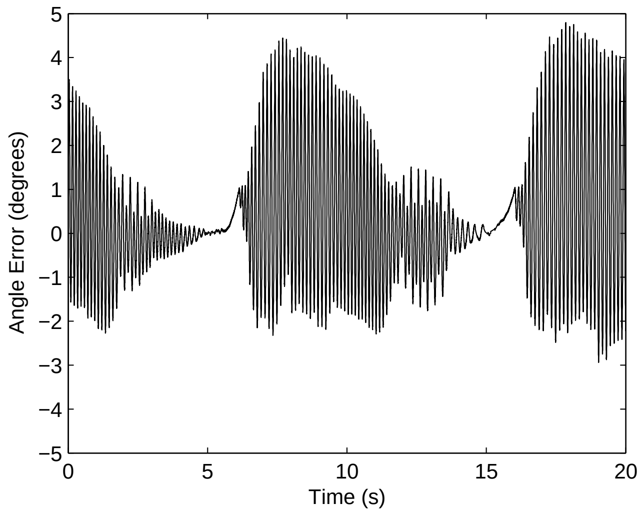

(a)

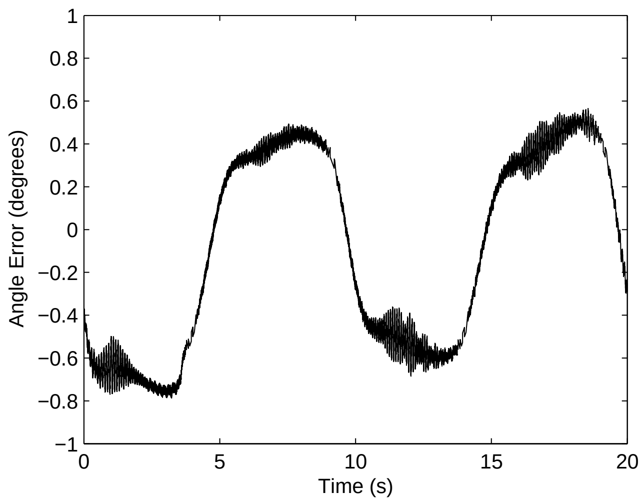

(b)

Figure 9: Output shaft angle error from the tracking response in Figure 6 with the relay controller (a), and the modified proportional controller (b).

actuators. This discontinuous switching between current levels is the main cause of limit cycles observed. In Figure 10(b), both actuators are supplied electric currents, albeit at different levels according to the modified proportional controller algorithm, to ensure that they are taut. The result is the reduced level of limit cycles observed.

Although not shown in this paper, similar results under the coupled condition had been recorded in our experiments. In those responses, the magnitude of the position error was found to have increased. This was due to the coupling effects of two antagonistic SMA pairs in motion.

In Figure 11, there is clearly an increase in the error magnitude as the frequency of the trajectory increases. Here the root-mean-square (RMS) error of the tracking responses under both uncoupled and coupled conditions are plotted together and compared. Note that the RMS error for the coupled system is the average of the RMS errors of the two individual pulleys. Results presented

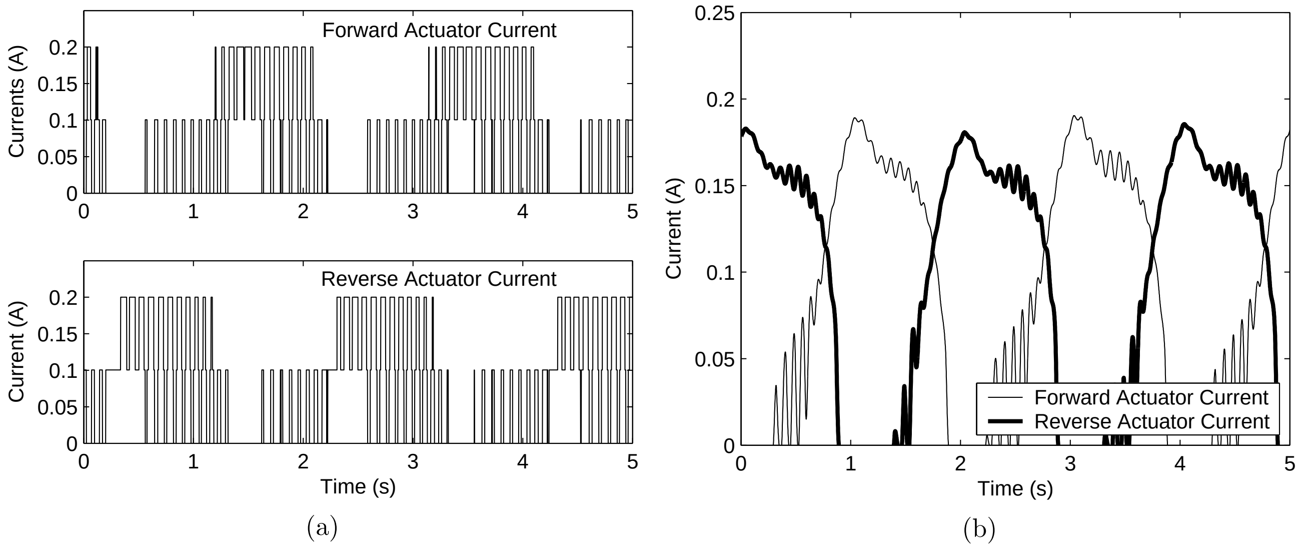

Figure 10: Actual current delivered to the two SMA wires actuating the pulley during the motion shown in Figure 7 with the relay controller (a), and the modified proportional controller (b).

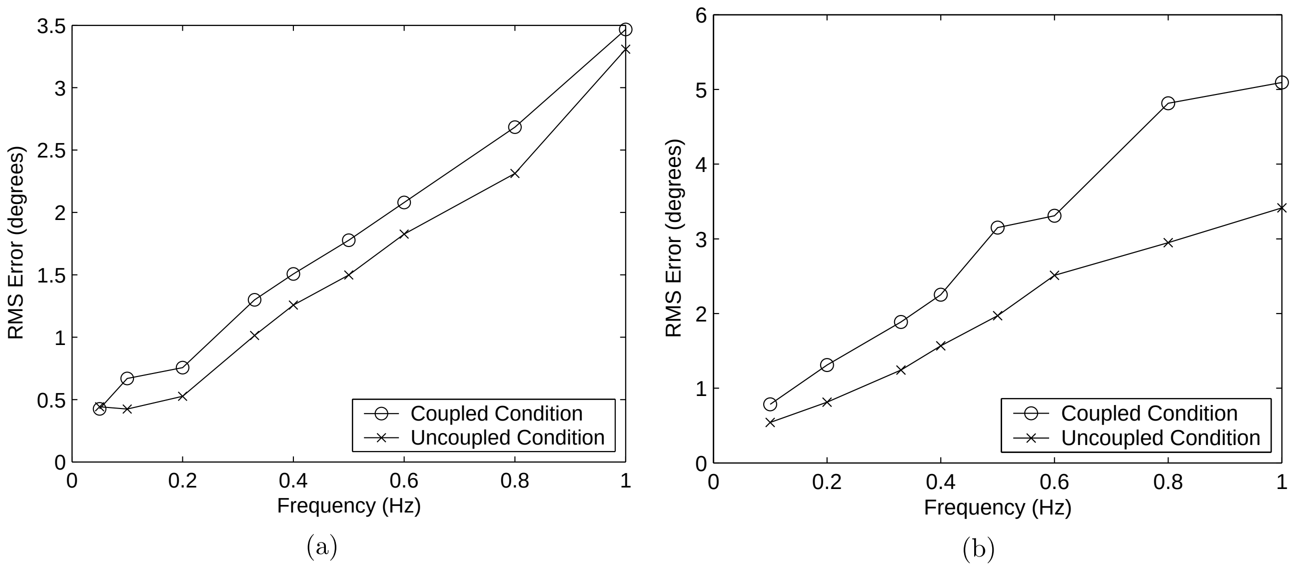

Figure 11: The RMS value of the angle error measured for a range of frequencies of the circular motion (a), and the square motion (b), of the 2-DOF pantograph using the modified proportional controller.

agree that the coupling between two actuator pairs has some impact on the accuracy and the limit cycle, resulting in the larger RMS errors compared to results with one pulley fixed.

In Figure 11(a), the 3.5° value of RMS error at 1 Hz tracking corresponds to approximately 12% of the rotation angle range of the circular motion. Although this is significantly better than the relay controller results, it is an indication that the modified proportional controller may not be the ideal controller for this SMA-actuated system. Figure 11(b) also presents the RMS error during the tracking of a square trajectory of the same size. The magnitudes of the RMS errors for square tracking are even larger compared to the circular tracking responses because of the higher speeds and accelerations that are required to track accurately.

Experiments with other trajectories, in various shapes and sizes, also yield results that follow the same observations as have been discussed in this paper.

4 Conclusion and Future Work

The experiments and results presented in this paper represents the first of its kind on the performance of a 2-DOF SMA-actuated robot. Results obtained for mechanisms based on only one antagonistic pair of SMA elements cannot be extended to explain the performance of the pantograph due to the coupling effect between antagonistic pairs of SMA actuators and the weight of the pantograph.

In this paper, two different controller designs have been implemented for the control of the pantograph under different conditions to demonstrate the trajectory tracking performance of the control system. Experimental results show that the modified proportional controller has an improved performance compared to the two-stage relay controller. The tracking accuracy has substantially improved with the elimination of large limit cycles problematic to relay control. The results also demonstrate that the 2-DOF SMA-actuated robot is capable of high speed response and relatively good tracking accuracy. One possibility of future work would be to compare the modified proportional controller with other published algorithms, such as in [Elahinia *et al.*, 2004].

We also believe that faster and more accurate response could be achieved with better controller design and implementation. We are planning to design and construct a new test rig with force sensors for measuring the stress on each SMA elements. Using data from the force sensors, we intend to implement better control systems for SMA actuators.

References

[Elahinia *et al.*, 2004] Mohammad H. Elahinia, T. Michael Seigler, Donald J. Leo and Mehdi Ahmadian. Nonlinear stress-based control of a rotary SMA-actuated manipulator. *Journal of Intelligent Material Systems and Structures*, 15(6):495-508, 2004.

[Featherstone and Teh, 2004] Roy Featherstone and Yee Harn Teh. Improving the speed of shape memory alloy actuators by faster electrical heating. In *Proceedings of the Ninth International Symposium on Experimental Robotics*, Paper ID 128, Singapore, June 2004.

[Grant, 1999] Danny Grant. Accurate and rapid control of shape memory alloy actuators. PhD Thesis TR-CIM-99-11, Centre for Intelligent Machines, McGill University, 1999.

[Ikuta *et al.*, 1988] Koji Ikuta, Masahiro Tsukamoto and Shigeo Hirose. Shape memory alloy servo actuator system with electric resistance feedback and application for active endoscope. In *Proceedings of the IEEE International Conference on Robotics and Automation*, pages 427-430, Philadelphia, PA, April 1988.

[Mosley and Mavroidis, 2001] Michael J. Mosley and Constantinos Mavroidis. Experimental nonlinear dynamics of a shape memory alloy wire bundle actuator. *Journal of Dynamic Systems, Measurement, and Control*, 123(1):103-112, 2001.

[Reynaerts and Van Brussel, 1998] Dominiek Reynaerts and Hendrik Van Brussel. Design aspects of shape memory actuators. *Mechatronics*, 8:635-656, 1998.

[Teh and Featherstone, 2004] Yee Harn Teh and Roy Featherstone. A new control system for fast motion control of SMA actuator wires. Submitted to *The First International Conference on Shape Memory and Related Technologies*, Paper ID 34, Singapore, November 2004.

[Troisfontaine *et al.*, 1998] N. Troisfontaine, Ph. Bidaud and P. Dario. Control experiments on two SMA based micro-actuators. In A. Casals & A. T. de Almeida (Eds.), *Experimental Robotics V*, pages 490-499. Springer, London, 1998.

[Yao *et al.*, 2004] Qin Yao, Sheng Jin and Pei-Sun Ma. The micro trolley based on SMA and its control system. *Journal of Intelligent and Robotic Systems*, 39:199-208, 2004.